Protein resistant oligo(ethylene glycol) terminated self-assembled monolayers of thiols on gold by vapor deposition in vacuum

Laxman Kankate, Udo Werner, Andrey Turchanin,[a] and Armin Gölzhäuser
Department of Physics, Physics of Supramolecular Systems and Surfaces, University of Bielefeld, 33615 Bielefeld, Germany

Helge Großmann and Robert Tampé
Institute of Biochemistry, Biocenter, Cluster of Excellence-Macromolecular Complexes, Johann Wolfgang Goethe-University, 60438 Frankfurt, Germany

(Received 19 February 2010; accepted 1 April 2010; published 27 April 2010)

Protein resistant oligo(ethylene glycol) (OEG) terminated self-assembled monolayers (SAMs) of thiols on gold are commonly used for suppression of nonspecific protein adsorption in biology and biotechnology. The standard preparation for these SAMs is the solution method (SM) that involves immersion of the gold surface in an OEG solution. Here the authors present the preparation of 11-(mercaptoundecyl)-triethylene glycol $[HS(CH_2)_{11}(OCH_2CH_2)_3OH]$ SAMs on gold surface by vapor deposition (VD) in vacuum. They compare the properties of SAMs prepared by VD and SM using x-ray photoelectron spectroscopy (XPS), polarization modulation infrared reflection absorption spectroscopy, and surface plasmon resonance measurements. VD and SM SAMs exhibit similar packing density and show a similar resistance to the nonspecific adsorption of various proteins (bovine serum albumin, trypsin, and myoglobin) under physiological conditions. A very high sensitivity of the OEG SAMs to x-ray radiation is found, which allows tuning their protein resistance. These results show a new path to *in situ* engineering, analysis, and patterning of protein resistant OEG SAMs by high vacuum and ultrahigh vacuum techniques. © *2010 American Vacuum Society.* [DOI: 10.1116/1.3407483]

I. INTRODUCTION

Surfaces that resist the nonspecific adsorption of proteins or cells are standard components for studies in proteomics,[1] cell biology,[2] as well as for applications in biotechnology.[3] Presently poly(ethylene glycol) (PEG) layers on solid substrate composed of long polymer chains are known to exhibit the best protein resistance (see, e.g., Ref. 4). However, also the densely packed oligo(ethylene glycol) (OEG) terminated self-assembled monolayers (SAMs) show a comparable to PEG protein resistance even if terminated with only short tri(ethylene glycol) chains.[5] Many studies of OEG terminated SAMs were conducted in the past years (see, e.g., Refs. 6–17) with the focus on understanding their structural properties and the reasons of their protein resistance. Although the mechanisms of the protein resistance have not yet been fully established, OEG terminated alkane thiol SAMs on gold have been used for suppression of nonspecific protein adsorption in biosensing,[18–21] cell adhesion studies,[2,22–24] fabrication of protein biochips,[25–29] and many other applications. In these studies OEG SAMs were prepared by self-assembly of molecules on a gold substrate immersed into an appropriate solution [solution method (SM)]. Although this preparation procedure seems rather simple, a lot of care must be taken of the cleanness of the utilized substrates and solvents and even SAMs prepared by similar protocols frequently show different characteristics and conformations of the OEG chains,[8,16] which are critical for their applications as protein resistive coatings. The solution method is also hard to combine with vacuum techniques used for processing and manufacturing of silicon based chips. Hence, an efficient fabrication of biochips that contain OEG SAMs is currently hampered by commonly used processing schemes.

Vapor deposition (VD) in vacuum is a standard method for the preparation of inorganic and organic coatings on solid surfaces for instance in molecular electronics (see, e.g., Ref. 30). In ultrahigh vacuum (UHV) the sample preparation parameters (e.g., cleanness of substrates and materials) can easily be controlled. Furthermore, the formed layers can be studied by *in situ* surface sensitive techniques enabling a comprehensive analysis of their structure and composition. Also the formed surfaces can be patterned *in situ* by electron beam lithography with a resolution below 10 nm,[31] which is of interest for nanofabrication. However, it is usually considered as difficult to form the self-assembled monolayers of thiols on gold by VD with a degree of quality sufficient for applications. The so-called kinetic traps, that are formations of the laying-down phase, resulting in SAMs with a low packing density, are discussed as a main problem.[32] Thus, presently most of the thiol SAMs are prepared by SM.

In this contribution we demonstrate the preparation of protein resistant 11-(mercaptoundecyl)-triethylene glycol $[HS(CH_2)_{11}(OCH_2CH_2)_3OH]$ SAMs on gold surfaces by VD in vacuum. To our knowledge this is the first study of VD for OEG terminated thiol SAMs on gold. We present a comparative analysis of SAMs prepared by VD and by SM using x-ray photoelectron spectroscopy (XPS), polarization modu-

[a]Electronic mail: turchanin@physik.uni-bielefeld.de

lation infrared reflection absorption spectroscopy (PM-IRRAS), and surface plasmon resonance (SPR) measurements. We show that the SAMs prepared by both methods have comparable packing density and resistance to the adsorption of various proteins (bovine serum albumin, trypsin, and myoglobin) under physiological conditions. Furthermore, we show the response of the SAMs to x-ray radiation. The obtained results indicate a new path for the engineering and analysis of biocompatible surfaces by vacuum techniques.

II. EXPERIMENT

A. Compounds and substrates

$HS(CH_2)_{11}(OCH_2CH_2)_3OH$ (abbreviation: $C_{11}EG_3OH$) compounds purchased from Sigma-Aldrich (95%) and Asemblon (99%) were utilized. XPS showed no differences in the quality of the SAMs made of compounds from both suppliers. At room temperature $C_{11}EG_3OH$ is in a liquid state.

Most of the XPS studies were conducted with $C_{11}EG_3OH$ SAMs prepared on 30 nm thick gold films thermally evaporated on Ti-primed silicon (100) wafers (G. Albert PVD coatings) with a rms roughness of ~1 nm and crystallite sizes below 50 nm with predominantly (111) orientation of the surface. For PM-IRRAS measurements, SAMs prepared on the similarly prepared gold films with a thickness of 100 nm (G. Albert PVD coatings) were used. SPR measurements were conducted on the self-made gold substrates prepared on precut glass slides (12×12 mm^2, 0.3 mm thick, borosilicate glass D263, PEO GmbH). Before gold evaporation substrates were cleaned in SC1 [standard cleaning solution 1:1 NH_3(25%)+1 H_2O_2(30%)+5 MilliQ] for 20 min, extensively rinsed with MilliQ and dried with N_2. A 2–5 nm adhesion layer of Cr and a 40–50 nm layer of Au were thermally evaporated in a Bal-Tec MED 020 vacuum coating system. XPS showed no differences in the quality of the SAMs prepared on the different gold substrates.

B. SAM preparation by VD in vacuum

VD and XPS of the samples were conducted *in situ*, i.e., without exposure to the ambient, in a multitechnique UHV instrument (see Ref. 33 for more details). Prior to VD gold substrates were cleaned by Ar-ion sputtering (1 kV, ~25 μA, and spot diameter ~20 mm) for a few minutes. The cleanness of the substrate was controlled by XPS. Immediately after cleaning, the gold surface was exposed to the molecular beam. A Knudsen-type organic evaporator (TCE-BSC, Kentax) was used for VD of SAMs on Au substrates placed inside the preparation chamber on a manipulator at RT. In order to obtain a reproducible molecular flux in different experimental runs, a fixed amount of liquid $C_{11}EG_3OH$ (~0.3 ml) was filled in a quartz crucible (orifice diameter of 3 mm). The material was evaporated at a constant temperature of 353 K (resulting in a pressure of $\sim5\times10^{-8}$ mbar measured by a N_2-calibrated ion gauge in the preparation chamber; the pressure before evaporation was typically $\sim5\times10^{-10}$ mbar) and the exposures were carried out by keeping the distance between the source and the substrate constant (~7 cm). Preceding the evaporation the material loaded into the evaporator was outgassed for at least 10 h at RT by an isolated pumping system.[33] The gate valve between the evaporator and the preparation chamber was opened immediately before the evaporation. Typical time for obtaining the maximum degree of coverage for $C_{11}EG_3OH$ SAMs at our experimental conditions was ~3 h. We estimated the corresponding exposure, correcting, similar to decanethiol,[34] the detected pressure by a sensitivity factor of 8. As found, an exposure of ~40 L (1 L$=10^{-6}$ Torr s) was typically sufficient to reach the maximum coverage of the SAM.

It is worth to note that in the course of our experiments we also tested the VD preparation of 16-mercaptohexadecanoic acid (triethylene glycol) ester SAMs,[25] which show protein resistant properties and were earlier utilized for the fabrication of protein biochips.[25,28] However, the VD of this, in comparison with $C_{11}EG_3OH$, much heavier compound was not possible. Evaporation temperatures below 400 K did not result in a vapor pressure sufficient for VD, whereas higher temperatures led to the thermal decomposition of the compound.

C. SAM preparation by SM

1. Protocol 1

Two solvents acetonitrile and ethanol were tested. Gold substrates were cleaned by UV/ozone, subsequently ultrasonicated in ethanol, and finally rinsed with the solvent used for SAM preparation. The cleaned substrates were immersed into the freshly prepared acetonitrile (HPLC grade) or ethanol (P.A. grade) based 1 mM $C_{11}EG_3OH$ solution for 24 h. Then the samples were ultrasonicated in acetonitrile (or ethanol) to remove the physisorbed layers. After drying with N_2 the samples were introduced into the UHV apparatus or directly characterized by PM-IRRAS. The XPS characterization showed that the preparation in acetonitrile[25] typically led to a higher effective thickness of the formed SAMs in comparison with the preparation in ethanol and, thus, was utilized in the following.

2. Protocol 2

Gold substrates were cleaned twice in SC1 [standard cleaning solution 1:1 NH_3(25%)+1 H_2O_2(30%) +5 MilliQ] for 20 min and extensively rinsed in MilliQ after each cleaning step. Subsequently, the substrate was rinsed in ethanol and acetonitrile for 1 min. The cleaned substrates were immersed into acetonitrile based 20 μM $C_{11}EG_3OH$ solution for 24 h. Afterward substrates were rinsed in acetonitrile and MilliQ including a treatment with ultrasonication for 3 min in each solvent. After drying with N_2 the samples were stored under Ar at 4 °C until they were used for the protein resistivity test.

D. XPS

The XPS data were recorded using a monochromatized Al x-ray source (1486.7 eV) and a hemispherical electron en-

ergy analyzer (Omicron, Sphera). To provide a precise energy calibration for the XPS binding energies, the Au $4f_{7/2}$ peak at 84.0 eV (Ref. 35) was used as a reference. The XPS data were measured at a photoelectron emission angle $\theta = 18°$ with an acceptance angle of 14° of the energy analyzer and an energy resolution of 0.9 eV. For the analysis of the XP spectra, a Shirley background subtraction and symmetric Voigt functions were used for fitting.[36] To determine the film thickness, the Au $4f_{7/2}$ signal intensity was assumed to be exponentially attenuated by the SAM overlayer of thickness d, according to $d = \lambda \cos\theta \ln(I_o(\text{Au } 4f_{7/2})/I(\text{Au } 4f_{7/2}))$, where $I_o(\text{Au } 4f_{7/2})$ and $I(\text{Au } 4f_{7/2})$ signals are the Au $4f_{7/2}$ intensities from the bare and SAM-covered gold surfaces, respectively. The photoelectron attenuation length, λ, was taken to be 36 Å.[8,27,37] The calculation of element ratios was conducted in frames of the statistical model.[36] The photoelectron attenuation lengths and sensitivity factors of C 1*s*/O 1*s* signals were taken to be 23.8/19.3 Å and 1/3.08, respectively.

E. PM-IRRAS

The infrared spectra were recorded using a nitrogen purged Bruker Vertex70 spectrometer with a PMA50 polarization modulator unit. The spectra were taken at an incident angle of 80° with a resolution of 4 cm^{-1}. Depending on the region of interest the photoelastic modulator was operated at 3000 or 1200 cm^{-1}, respectively. Typical measurement time was about 10 min. As reference samples, hexadecane thiol (Sigma-Aldrich, 95%) SAMs incubated at room temperature on gold substrates in 1 mM ethanol solution for 24 h were measured. For these samples asymmetric C–H stretching modes of the alkyl chains (ν_a) were typically observed at ~2919 cm^{-1}.

F. SPR measurements

Measurements were performed in a Biacore T100 (GE Healthcare) at a flow rate of 10 μl/min. Substrates were mounted on the sample holder using double-sided tape. Bovine serum albumine (Roth), Trypsin (Merck), and Myoglobin (Sigma) were dissolved in HBS (HEPES buffered saline: 20 mM HEPES, 150 mM NaCl, prepared in MilliQ, *p*H 7.5) at 1 and 5 mg/ml. Each measurement was composed of the following steps: (i) 1800 s equilibration with running buffer (HBS), (ii) injection of a 1 mg/ml protein solution for 600 s followed by a dissociation phase of 300 s, (iii) injection of a 5 mg/ml protein solution for 600 s followed by a dissociation phase of 300 s, and (iv) injection of a NaCl standard solutions (0.4 M in HBS). Steps (i) and (iv) were performed in all four flow channels, while in steps (ii) and (iii) one flow channel was dedicated to one protein solution. To quantify the level of nonspecific protein adhesion the SPR signal differences were calculated at defined time points before ($t_1 = 250$ s) and after ($t_2 = 1150$ s) the injection of the proteins. Because of possible thickness variations in the Au layer on each sample, all values were normalized with the SPR signal shift generated by the NaCl standard solution.

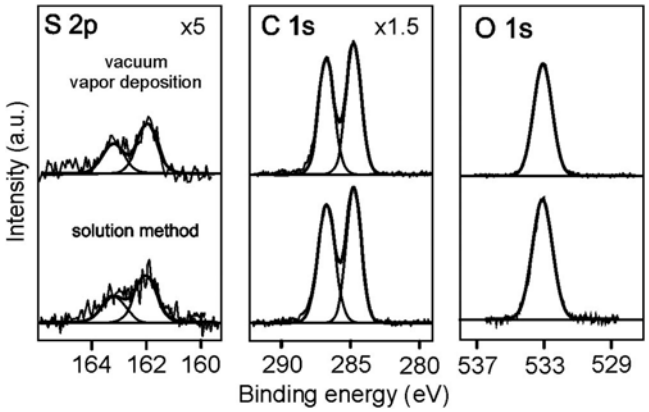

FIG. 1. XP spectra of $C_{11}EG_3OH$ SAMs on gold prepared by VD in vacuum and by SM. The S 2*p* and C 1*s* spectra for both VD and SM SAMs were expanded by factors ×5 and ×1.5, respectively. VD conditions: Source and surface temperatures were 353 and 300 K, respectively. The time of deposition was 3 h. SM conditions: Acetonitrile based 1 mM solution was used (protocol 1); the incubation time was 24 h. Polycrystalline Au (30 nm)/Si substrates were utilized. For more details, see Sec. II.

III. RESULTS AND DISCUSSION

A. XPS characterization

Figure 1 shows the XP spectra of $C_{11}EG_3OH$ SAMs on gold with the maximum achievable coverage as prepared by solution method and by vapor deposition in vacuum. As can be seen, both preparation methods lead to rather similar spectra. The S 2*p* signals show a doublet at a binding energy (BE) of ~162.0 eV with a spin-orbit splitting of 1.2 eV and a 2:1 branching ratio between the S $2p_{3/2}$ and S $2p_{1/2}$ components as expected for a monolayer of thiolates on gold.[38] The full width at half maximum (FWHM) of the sulfur peaks corresponds to ~0.9 eV. No additional sulfur species were observed excluding the formation of unbounded (physisorbed) thiols, disulfides [BE of ~163.5 eV (Refs. 33 and 39)] or oxidized sulfur species [BE of ~168.0 eV (Ref. 40)]. The C 1*s* signal consists of two components with the BEs of ~284.8 eV, C 1*s*(I), and ~286.8 eV, C 1*s*(II), accounting for carbon atoms in the alkyl chains and in the tri(ethylene glycol) groups,[27] respectively. The O 1*s* signal demonstrates a BE of ~533.1 eV which is typical for OEG groups.[16,27] The C 1*s*(II)/O 1*s* ratios (areas under the corresponding peaks were considered) calculated from the spectra within the statistical model[36] showed typical values of about 6:3.5 that are close to the expected stoichiometric ratio of 6:4 (Table I).

The "upright" orientation of the molecules and the surface location of the tri(ethylene glycol) groups of $C_{11}EG_3OH$ SAMs prepared by both methods can clearly be deduced from the C 1*s*(I)/C 1*s*(II) ratios, which were about 11:10 and 11:12 for the VD SAMs and SM SAMs, respectively, whereas their stoichiometric ratio is 11:4 (Table I). The observed C 1*s*(I)/C 1*s*(II) ratios varied from sample to sample by ~10% for both preparation methods. From the attenuation of the Au 4*f* signal (not shown), the effective thickness of VD SAMs was found to be 19.0 ± 1.5 Å. The effective thickness of SM SAMs was ~1 Å lower. These values are

TABLE I. Binding energies (FWHM values in brackets) in eV, and C 1*s*(I)/C 1*s*(II) and C 1*s*(II)/O 1*s* intensity ratios of the characteristic XP signals for $C_{11}EG_3OH$ SAMs prepared by VD and SM. C 1*s*(I) and C 1*s*(II) signals account for carbon atoms in the alkyl chains and in the tri(ethylene glycol) groups.

Method/signal	S $2p_{3/2,1/2}$	C 1*s*(I)	C 1*s*(II)	O 1*s*	C 1*s*(I)/C 1*s*(II)	C 1*s*(II)/O 1*s*
VD	162.0 (0.9) 163.2 (0.9)	284.8 (1.3)	286.8 (1.3)	533.1 (1.3)	11:10	6:3.5
SM	162.0 (0.9) 163.2 (0.9)	284.8 (1.1)	286.8 (1.5)	533.1 (1.5)	11:12	6:3.5

in a good agreement with the thickness of an ideal $C_{11}EG_3OH$ SAM on gold (~23 Å) assuming a tilt angle of the alkyl chains of 30° with respect to the surface normal and a helical conformation of the OEG groups.[8] A somewhat lower thickness of the SAM may account for structural defects (*gauche* defects in alkyl chains or grain boundaries) in the SAM, different than helical conformation of OEG groups (see PM-IRRAS section), a possible uncertainty in the value of the inelastic mean free path for Au 4*f* electrons, and the x-ray induced damage of the monolayer (see Sec. III B).

Despite of the rather similar character of the XP spectra for $C_{11}EG_3OH$ SAMs prepared by VD and SM, we observed systematic differences in the FWHM values of the C 1*s*(I), C 1*s*(II), and O 1*s* signals (Table I). For SM SAMs the FWHM value of the C 1*s*(I) signal was ~1.1 eV, whereas for VD SAMs this value was ~1.3 eV. The FWHM values of the C 1*s*(II) signal were ~1.5 eV and ~1.3 eV for SM and VD SAMs, respectively. This difference in the carbon signal of OEG groups correlates with the FWHM values of the O 1*s* signal which were ~1.5 eV for SM SAMs and ~1.3 eV for VD SAMs. Thus, the width of the spectral features due to alkyl chains is narrower for SM SAMs, whereas the width of the spectral features due to OEG groups is narrower for VD SAMs. These results are indicative for structural and conformation differences in both SAMs and suggest a higher degree of order in the alkane chains and a lower degree of order in the OEG groups for SM SAMs in comparison with VD SAMs. We show that this structural analysis is in good agreement with the results of our infrared spectroscopy study (see Sec. III C).

B. X-ray induced modification

Secondary electrons generated by the sample substrate[41] and by nonmonochromatic x-ray sources are usually considered as a main reason for the degradation of organic monolayers on solid substrates during XPS experiments. Although our XPS study was conducted with a monochromatic source, which strongly reduces the amount of secondary electrons, a degradation of $C_{11}EG_3OH$ SAMs was nevertheless observed. Figure 2 shows the normalized intensities of the C 1*s*(I), C 1*s*(II), and O 1*s* signals for a VD SAM as a function of the x-ray exposure time as determined after subsequent XP scans. The normalization was conducted to the signal intensities after the first scan. As can be seen, all signals show a gradual decrease in the intensities as a function of the exposure time and reach after five subsequent XP scans about 95% and 70% of the magnitudes for alkyl [C 1*s*(I)] and OEG chains [C 1*s*(II) and O 1*s*], respectively. The effective thickness of the monolayer reduces to ~15 Å. The time evaluation of the effective thickness (not shown) is linear. This dependence suggests that even the first XP spectrum, Fig. 1, is affected by radiation damage, and the reduction in the SAM thickness by ~1 Å is expected. The XPS data show that the intensity of XP signals of the OEG groups decreases faster than the intensity of the alkyl chains, Fig. 2, which may be indicative for the faster degradation of the OEG groups in comparison to the alkyl chains. We also observed that by proceeding x-ray irradiation, similar to the alkane thiols SAMs on gold,[42] a second S 2*p* doublet forms at a BE of ~163.5 eV. This doublet most likely accounts for the formation of organosulfides.[43,44] Finally, we note that $C_{11}EG_3OH$ SAMs from solution have a similar response to x-ray irradiation as VD SAMs. The observed degradation of $C_{11}EG_3OH$ SAMs after XPS measurements strongly influences the protein resistivity of these monolayers (see Sec. III D).

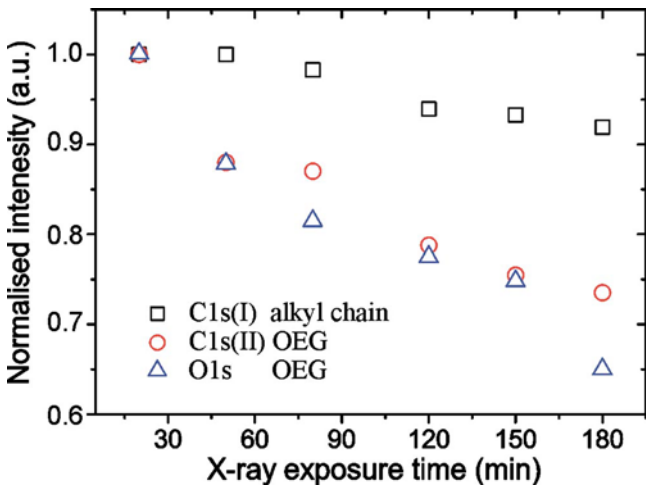

FIG. 2. (Color online) X-ray induced modification of $C_{11}EG_3OH$ SAMs on gold prepared by vapor deposition as a function of radiation dose. Intensities of C 1*s*(I) (alkyl chains) and C 1*s*(II), O 1*s* (OEG groups) as a function of x-ray exposure time (x-ray source parameters: mono-Al $K\alpha$, 225 W). The effective thickness of the SAM after ~20 min of exposure, the time which is necessary for a complete acquisition of high resolution XP spectra of Au 4*f*, S 2*p*, C 1*s*, and O 1*s* signals at our experimental conditions, is ~20 Å. The effective thickness of ~15 Å was detected after ~180 min of exposure.

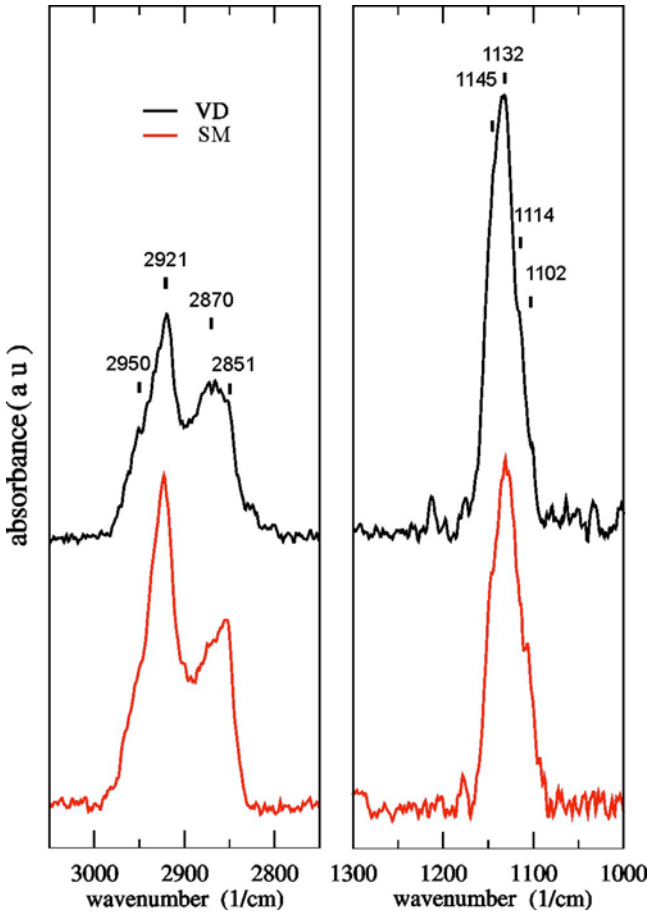

FIG. 3. (Color online) PM-IRRAS spectra of $C_{11}EG_3OH$ SAMs on gold prepared by VD in vacuum and by SM. Characteristic C–H (left) and C–O–C (right) stretching regions. For SAM preparation conditions, see Fig. 1. Polycrystalline Au (100 nm)/Si substrates were utilized.

C. PM-IRRAS characterization

Figure 3 shows the PM-IRRAS spectra of VD and SM $C_{11}EG_3OH$ SAMs of the characteristic[8] C–H and C–O–C stretching regions. In agreement with the XPS results the PM-IRRAS data also confirm a comparable quality of the SAMs prepared by both methods. The assignment and analysis of the observed infrared active modes were conducted on the basis of published data for various OEG terminated alkane thiols SAMs on gold.[8,11,16]

The asymmetric (ν_a) and symmetric (ν_s) C–H stretching modes of alkyl chains were detected at ~2921 and ~2851 cm^{-1}, whereas the ν_a and ν_s C–H stretching modes of the OEG part were found at ~2950 and ~2870 cm^{-1}, Fig. 3. The observation of the alkyl ν_a peak at ~2921 cm^{-1} suggests the presence of a substantial degree of *gauche* defects, i.e., disorder, in the alkyl chains of the formed SAMs. For alkane thiol SAMs on gold with a higher degree of crystallinity this peak is expected at ~2917 cm^{-1}.[45,46] A shift of the ν_a of alkyl chains to higher frequencies was observed in OEG terminated alkane thiol SAMs upon increasing the temperature and was related to an increase in the population of *gauche* defects along the alkyl chains.[47] The appearance of the ν_s peak of OEG groups at ~2870 cm^{-1} is characteristic for their amorphous-like conformation. This conclusion is in agreement with the position of the C–O–C stretch peaks centered at ~1132 cm^{-1}.[8,11] Besides a very strong peak at ~1132 cm^{-1} the weaker shoulders of the C–O–C skeleton modes at 1102, 1114, and 1145 cm^{-1} are also recognized in Fig. 3, which is indicative of the presence of some amount of all-trans and helical configuration of the OEG groups in a SAM.[8,11,16]

Finally, the comparative analysis of the PM-IRRAS spectra shows some differences between VD and SM SAMs. For VD SAMs the position of the C–O–C stretch peak was typically observed at ~1132 cm^{-1} and the intensity ratio (maximum intensity values were considered) between the C–O–C stretch and the ν_a of alkyl chains, C–O–C/C–H, was detected at about 2. For SM SAMs larger variations between different samples were observed: The position of the C–O–C stretch varied from 1130 to 1140 cm^{-1} and the C–O–C/C–H ratio ranged from 1.1 to 2. Thus the preparation of $C_{11}EG_3OH$ SAMs by VD leads to more reproducible results. Since the ν_a intensity of alkyl chains depends strongly on their tilt angle and the amount of *gauche* defects,[47] the variation in the C–O–C/C–H ratio for SM SAMs is indicative for their structural dissimilarities. Although the infrared spectroscopy data show that alkyl chains in both VD and SM SAMs have low crystallinity, the narrower width for the XP peak of alkyl chains in SM SAMs, as described earlier, suggests a somewhat higher ordering in comparison to VD SAMs. In addition, a specific conformation of the OEG chain seems to be more characteristic for VD SAMs. Both the lower width of the O 1*s* and C 1*s*(II) XP peaks as well as the stable position (~1132 cm^{-1}) of the C–O–C stretching of VD SAMs in comparison with SM SAMs support this conclusion.

We attribute the described differences between alkyl and OEG chains of VD and SM SAMs to the different kinetics and equilibration dynamics during the self-assembly at the gas/solid and liquid/solid interfaces. The formation of alkanethiols at the liquid/solid interface of gold was studied by various techniques (for reviews, see, e.g., Refs. 48 and 49) that revealed the complexity of the process which can proceed stepwise and depend on the molecular structure of the self-assembling thiol, type of the utilized solvent, as well as on concentration and temperature. Different steps in the formation of a SAM were identified by infrared-visible sum frequency spectroscopy.[50] In an initial fast step the Au–S bonds are formed. In subsequent steps with much slower time constants, neighboring alkane chains align to form a well ordered monolayer. During VD at the gas/solid interface, this slower ordering process may be kinetically hindered, leading to less ordered alkane chains exhibiting more *gauche* defects. Instead, this may allow more interaction of neighboring OEG units leading to their better relaxation in comparison to the self-assembly from solvent, where alkane chains are more ordered.

D. Protein resistance tests by SPR

To study the protein resistance of VD and SM SAMs, SPR experiments were performed. Three different protein so-

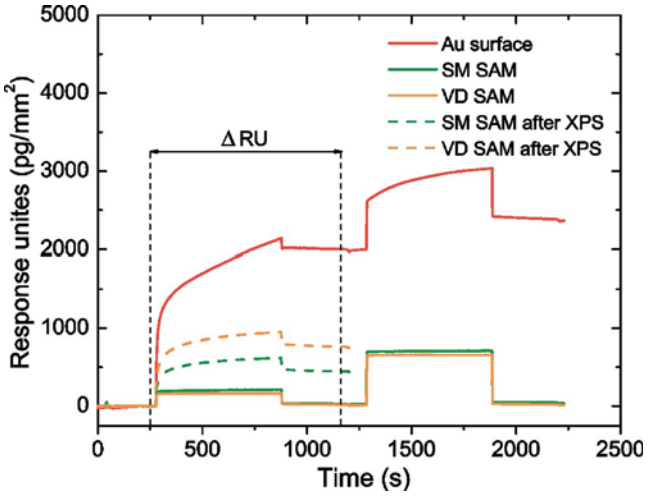

FIG. 4. (Color online) SPR characterization of the protein resistance of VD and SM $C_{11}EG_3OH$ SAMs. Measurements with two different concentrations of BSA on a bare Au/glass surface, VD, and SM SAMs. While on the bare Au/glass surface BSA adsorbs, as is evident from the characteristic curve and the higher signal after the injection, both SAMs are almost completely protein repellent, showing only the refractive index shift of the injected solution. Dashed vertical lines indicate time points at which the signal difference ΔRU was calculated in order to quantify the amount of adsorbed protein. VD SAMs were prepared as described in Fig. 1. SM SAMs were prepared by using protocol 2 (see Sec. II). Dashed curves correspond to the samples exposed to x rays (BSA concentration of 1 mg/ml).

lutions [containing bovine serum albumine (BSA), trypsin, or myoglobin], each with a concentration of 1 mg/ml, were flown over the surfaces at a rate of 10 μl/min. To measure the quality of SAMs in terms of protein resistance we also included a bare Au/glass substrate. To quantify the level of nonspecific protein adsorption, we measured the SPR signal before and after the injection of the proteins.

Figure 4 shows the results for BSA. Upon the injection of the protein onto the bare Au surface, a strong shift of the SPR response was observed. Two components of this shift can be distinguished: The first, immediate one, is due to the higher refractive index of the protein solution compared to the refractive index of the running buffer; the second one, which is slower and which shows a characteristic curvature, is caused by the adsorption of proteins onto the Au surface. After the injection is stopped and the running buffer is flown over the surface again, the SPR signal rapidly decreases, which, again, is based on the refractive index change in the solutions. It then remains at a level of about 2000 RU (response units) higher than that before the injection, indicating an increase in surface mass of about 2 ng/mm^2 of adsorbed protein. A subsequent injection of a solution containing five times as much protein further increases the signal to 2400 RU. The mass increase after the second injection is much lower, which suggests that most of the binding sites were already occupied and the surface coverage is nearly saturated.

The above experiments were repeated for VD and SM SAMs, which were prepared on thin gold films on glass substrates. The most obvious difference in SAMs compared to the bare Au surface is a rectangular signal progression without a clear binding kinetics during the first injection. Only the refractive index shift upon injection of the protein solution could be observed. When the injection was stopped, the signal returned nearly to its initial value, stabilizing at around 30 RU. Thus, only a very small amount of BSA remained on the SAM surfaces. Both SAMs showed almost the same protein resistance. To further quantify these properties we calculated the signal differences (ΔRU) before and after the first injection for each surface and for each protein. Since all gold on glass substrates were self-made, a variation in gold thickness cannot be excluded, thus the RU values for the measured samples had to be normalized. To this end the signal shift of a 0.4 M NaCl solution was measured on all surfaces and used as a reference for the signals measured during protein injection. The results are shown in Table II. Compared to the bare Au surface the percentage of nonspecific adsorption of the tested proteins was between 1% and 3% on both VD and SM SAMs, demonstrating their equivalent quality with respect to the protein resistance.

TABLE II. Normalized values of ΔRU before and after the protein injection. Values in parentheses represent percentages of nonspecific protein adsorption with respect to the plain Au surface without a SAM.

Protein	Plain Au (RU)[a]	SM SAM (RU)[a]	VD SAM (RU)[a]
BSA	2000.72	19.74 (0.99%)	32.62 (1.63%)
Trypsin	1089.69	11.11 (1.02%)	25.94 (2.38%)
Myoglobin	1991.41	49.88 (2.51%)	27.89 (1.40%)

[a]RU is the response units (pg/mm^2).

Finally, note that x-ray irradiation of VD and SM SAMs has a strong influence on the protein resistance of the monolayers, Fig. 4. Even after ~30 min of x-ray irradiation, the time which is necessary for a complete acquisition of XP spectra at our experimental conditions, the protein resistance of $C_{11}EG_3OH$ SAMs is strongly diminished. These results suggest that in the first place the OEG groups, which are responsible for the protein resistive properties, are influenced by x-ray irradiation. Since the XPS analysis suggests a reasonable stoichiometry and an effective thickness of $C_{11}EG_3OH$ SAMs, we conclude that the protein resistance demonstrates a delicate balance between the amount of available ethylene glycol groups (see Fig. 2) and the ability to resist the nonspecific protein adsorption. Thus, the tuning of protein resistance by extreme UV and by electron induced modification of OEG terminated SAMs[51,52] opens a new pathway for lithography of bioactive surfaces with a lateral resolution of periodic features down to the nanoscale.[53]

IV. SUMMARY AND CONCLUSIONS

In this contribution we have demonstrated the preparation and characterization of protein resistive OEG terminated SAMs of thiols on gold by VD in vacuum. The prepared $C_{11}EG_3OH$ SAMs form a "standing-up" phase and have a similar packing density as the SAMs prepared by standard SM. A comparative XPS and PM-IRRAS analysis shows some structural differences in the monolayers formed by both methods. The VD SAMs in comparison with SM SAMs

demonstrate a somewhat lower ordering of the alkyl chains and more stable (amorphous) configuration of the OEG chains that is most likely caused by the different kinetics and equilibration dynamics during the self-assembly at the gas/solid and liquid/solid interfaces. The protein resistive properties of the SAMs prepared by both methods, as studied by SPR measurements of three different proteins (BSA, trypsin, and myoglobin) were found to be very similar. We have found that the OEG terminated SAMs have a strong response to the x-ray (electron) irradiation, which causes the prevailing damage of the OEG groups. This radiation induced modification can be utilized for tuning the protein resistance. Finally, we note that the fabrication of the protein resistant SAMs at vacuum conditions is favorable to the analysis of these monolayers with different surface sensitive methods operating only at ultrahigh vacuum conditions and, thus, can have a strong impact on the further understanding of their properties. On the other hand, the vacuum preparation of $C_{11}EG_3OH$ SAMs is compatible with the utilization of electron beam lithography, which, in combination with the shown radiation response, is of great potential for the fabrication of bioactive micro- and nanopatterns in biochip technology.

ACKNOWLEDGMENT

The authors thank the German Ministry for Education and Research (BMBF) for support through the Program "Nanobiotechnology" Grant BiNaTemp.

[1]D. S. Wilson and S. Nock, Curr. Opin. Chem. Biol. **6**, 81 (2002).
[2]P. P. Girard, E. A. Cavalcanti-Adam, R. Kemkemer, and J. P. Spatz, Soft Matter. **3**, 307 (2007).
[3]J. C. Love, L. A. Estroff, J. K. Kriebel, R. G. Nuzzo, and G. M. Whitesides, Chem. Rev. (Washington, D.C.) **105**, 1103 (2005).
[4]P. Kingshott and H. J. Griesser, Curr. Opin. Solid State Mater. Sci. **4**, 403 (1999).
[5]C. Pale-Grosdemange, E. S. Simon, K. L. Prime, and G. M. Whitesides, J. Am. Chem. Soc. **113**, 12 (1991).
[6]K. L. Prime and G. M. Whitesides, Science **252**, 1164 (1991).
[7]R. L. C. Wang, H. J. Kreuzer, and M. Grunze, J. Phys. Chem. B **101**, 9767 (1997).
[8]P. Harder, M. Grunze, R. Dahint, G. M. Whitesides, and P. E. Laibinis, J. Phys. Chem. B **102**, 426 (1998).
[9]R. Valiokas, S. Svedhem, S. C. T. Svensson, and B. Liedberg, Langmuir **15**, 3390 (1999).
[10]M. Zolk, F. Eisert, J. Pipper, S. Herrwerth, W. Eck, M. Buck, and M. Grunze, Langmuir **16**, 5849 (2000).
[11]R. Valiokas, S. Svedhem, M. Ostblom, S. C. T. Svensson, and B. Liedberg, J. Phys. Chem. B **105**, 5459 (2001).
[12]S. Herrwerth, W. Eck, S. Reinhardt, and M. Grunze, J. Am. Chem. Soc. **125**, 9359 (2003).
[13]L. Y. Li, S. F. Chen, J. Zheng, B. D. Ratner, and S. Y. Jiang, J. Phys. Chem. B **109**, 2934 (2005).
[14]R. Valiokas, M. Ostblom, F. Bjorefors, B. Liedberg, J. Shi, and P. Konradsson, BioInterphases **1**, 22 (2006).
[15]M. W. A. Skoda, R. M. J. Jacobs, J. Willis, and F. Schreiber, Langmuir **23**, 970 (2007).
[16]R. Valiokas *et al.*, J. Electron Spectrosc. Relat. Phenom. **172**, 9 (2009).
[17]S. Schilp, A. Rosenhahn, M. E. Pettitt, J. Bowen, M. E. Callow, J. A. Callow, and M. Grunze, Langmuir **25**, 10077 (2009).
[18]J. Lahiri, L. Isaacs, J. Tien, and G. M. Whitesides, Anal. Chem. **71**, 777 (1999).
[19]Q. M. Yu, S. F. Chen, A. D. Taylor, J. Homola, B. Hock, and S. Y. Jiang, Sens. Actuators B **107**, 193 (2005).
[20]A. Larsson, J. Angbrant, J. Ekeroth, P. Mansson, and B. Liedberg, Sens. Actuators B **113**, 730 (2006).
[21]X. H. Lou and L. He, Sens. Actuators B **129**, 225 (2008).
[22]M. Mrksich, Curr. Opin. Colloid Interface Sci. **2**, 83 (1997).
[23]B. T. Houseman and M. Mrksich, Biomaterials **22**, 943 (2001).
[24]S. Schilp, A. Kueller, A. Rosenhahn, M. Grunze, M. E. Pettitt, M. E. Callow, and J. A. Callow, BioInterphases **2**, 143 (2007).
[25]A. Tinazli, J. L. Tang, R. Valiokas, S. Picuric, S. Lata, J. Piehler, B. Liedberg, and R. Tampe, Chem.-Eur. J. **11**, 5249 (2005).
[26]A. Biebricher, A. Paul, P. Tinnefeld, A. Gölzhäuser, and M. Sauer, J. Biotechnol. **112**, 97 (2004).
[27]A. Turchanin, M. Schnietz, M. El-Desawy, H. H. Solak, C. David, and A. Gölzhäuser, Small **3**, 2114 (2007).
[28]A. Turchanin, A. Tinazli, M. El-Desawy, H. Großmann, M. Schnietz, H. H. Solak, R. Tampé, and A. Gölzhäuser, Adv. Mater. (Weinheim, Ger.) **20**, 471 (2008).
[29]P. Jonkheijm, D. Weinrich, H. Schroder, C. M. Niemeyer, and H. Waldmann, Angew. Chem., Int. Ed. **47**, 9618 (2008).
[30]G. Witte and C. Wöll, J. Mater. Res. **19**, 1889 (2004).
[31]M. J. Lercel, H. G. Craighead, A. N. Parikh, K. Seshadri, and D. L. Allara, Appl. Phys. Lett. **68**, 1504 (1996).
[32]F. Schreiber, Prog. Surf. Sci. **65**, 151 (2000).
[33]L. Kankate, A. Turchanin, and A. Gölzhäuser, Langmuir **25**, 10435 (2009).
[34]A. Eberhardt, P. Fenter, and P. Eisenberger, Surf. Sci. **397**, L285 (1998).
[35]NIST X-ray Photoelectron Spectroscopy Database 20, Version 3.4, Web Version, 2003.
[36]D. Briggs and J. T. Grant, *Surface Analyses by Auger and X-Ray Photoelectron Spectroscopy* (SurfaceSpectra Limited, Chichester, 2003).
[37]P. E. Laibinis, C. D. Bain, and G. M. Whitesides, J. Phys. Chem. **95**, 7017 (1991).
[38]M. Zharnikov and M. Grunze, J. Phys.: Condens. Matter **13**, 11333 (2001).
[39]D. G. Castner, K. Hinds, and D. W. Grainger, Langmuir **12**, 5083 (1996).
[40]M. J. Tarlov, D. R. F. Burgess, and G. Gillen, J. Am. Chem. Soc. **115**, 5305 (1993).
[41]P. E. Laibinis, R. L. Graham, H. A. Biebuyck, and G. M. Whitesides, Science **254**, 981 (1991).
[42]M. Zharnikov, W. Geyer, A. Gölzhauser, S. Frey, and M. Grunze, Phys. Chem. Chem. Phys. **1**, 3163 (1999).
[43]K. Heister, M. Zharnikov, M. Grunze, L. S. O. Johansson, and A. Ulman, Langmuir **17**, 8 (2001).
[44]A. Turchanin, D. Käfer, M. El-Desawy, C. Wöll, G. Witte, and A. Gölzhäuser, Langmuir **25**, 7342 (2009).
[45]M. D. Porter, T. B. Bright, D. L. Allara, and C. E. D. Chidsey, J. Am. Chem. Soc. **109**, 3559 (1987).
[46]R. G. Nuzzo, L. H. Dubois, and D. L. Allara, J. Am. Chem. Soc. **112**, 558 (1990).
[47]R. Valiokas, M. Ostblom, S. Svedhem, S. C. T. Svensson, and B. Liedberg, J. Phys. Chem. B **106**, 10401 (2002).
[48]D. K. Schwartz, Annu. Rev. Phys. Chem. **52**, 107 (2001).
[49]M. Buck, and M. Himmelhaus, J. Vac. Sci. Technol. A **19**, 2717 (2001).
[50]M. Himmelhaus, F. Eisert, M. Buck, and M. Grunze, J. Phys. Chem. B **104**, 576 (2000).
[51]M. Schnietz and A. Turchanin, Paul Scherrer Institute Scientific Report to SLS Proposal No. 20070440, 2007.
[52]N. Ballav, H. Thomas, T. Winkler, A. Terfort, and M. Zharnikov, Angew. Chem., Int. Ed. **48**, 5833 (2009).
[53]V. Auzelyte *et al.*, J. Micro/Nanolith. MEMS MOEMS **8**, 021204 (2009).